© 2015. Published by The Company of Biologists Ltd | Development (2015) 142, 1553 doi:10.1242/dev.124214

CORRECTION

The Rac1 regulator ELMO controls basal body migration and docking in multiciliated cells through interaction with Ezrin

Daniel Epting, Krasimir Slanchev, Christopher Boehlke, Sylvia Hoff, Niki T. Loges, Takayuki Yasunaga, Lara Indorf, Sigrun Nestel, Soeren S. Lienkamp, Heymut Omran, E. Wolfgang Kuehn, Olaf Ronneberger, Gerd Walz and Albrecht Kramer-Zucker

There was an error published in *Development* **142**, 174-184.

In the supplementary material (mRNA and morpholino injection) the morpholino SB-MO *dock1* was incorrectly listed as: 5′-ACACTCTAGTGAGTATAGTGTGCAT-3′. The correct sequence is: 5′-ACCATCCTGAGAAGAGCAAGAAATA-3′ (corresponding to MO4-dock1 in ZFIN).

The authors apologise to readers for this mistake.

© 2015. Published by The Company of Biologists Ltd | Development (2015) 142, 174-184 doi:10.1242/dev.112250

RESEARCH ARTICLE

The Rac1 regulator ELMO controls basal body migration and docking in multiciliated cells through interaction with Ezrin

Daniel Epting[1], Krasimir Slanchev[1], Christopher Boehlke[1], Sylvia Hoff[1], Niki T. Loges[2], Takayuki Yasunaga[1], Lara Indorf[1], Sigrun Nestel[3], Soeren S. Lienkamp[1,4], Heymut Omran[2], E. Wolfgang Kuehn[1,4], Olaf Ronneberger[4,5], Gerd Walz[1,4] and Albrecht Kramer-Zucker[1,*]

ABSTRACT

Cilia are microtubule-based organelles that are present on most cells and are required for normal tissue development and function. Defective cilia cause complex syndromes with multiple organ manifestations termed ciliopathies. A crucial step during ciliogenesis in multiciliated cells (MCCs) is the association of future basal bodies with the apical plasma membrane, followed by their correct spacing and planar orientation. Here, we report a novel role for ELMO-DOCK1, which is a bipartite guanine nucleotide exchange factor complex for the small GTPase Rac1, and for the membrane-cytoskeletal linker Ezrin, in regulating centriole/basal body migration, docking and spacing. Downregulation of each component results in ciliopathy-related phenotypes in zebrafish and disrupted ciliogenesis in *Xenopus* epidermal MCCs. Subcellular analysis revealed a striking impairment of basal body docking and spacing, which is likely to account for the observed phenotypes. These results are substantiated by showing a genetic interaction between *elmo1* and *ezrin b*. Finally, we provide biochemical evidence that the ELMO-DOCK1-Rac1 complex influences Ezrin phosphorylation and thereby probably serves as an important molecular switch. Collectively, we demonstrate that the ELMO-Ezrin complex orchestrates ciliary basal body migration, docking and positioning *in vivo*.

KEY WORDS: Ciliogenesis, ELMO, DOCK1, Rac1, Ezrin, Multiciliated cells, *Xenopus*, Zebrafish

INTRODUCTION

Mutations in genes that impair ciliogenesis are implicated in complex human diseases collectively termed ciliopathies (Hildebrandt et al., 2011). Cilia are microtubule-based organelles and commonly divided into primary non-motile and motile cilia (Goetz and Anderson, 2010); the cilia of multiciliated cells (MCCs) are typically motile. Ciliogenesis in MCCs is initiated by the *de novo* generation of centrioles within the cytoplasm, followed by their migration to the apical cell membrane where they mature into basal bodies (Steinman, 1968; Dawe et al., 2007; Klos Dehring et al., 2013). The transport of the future basal bodies to the apical cell membrane requires an intact actin cytoskeleton and involves actin-myosin-based mechanisms (Lemullois et al., 1988; Boisvieux-Ulrich et al., 1990). The apical cell membrane in MCCs contains a network of actin filaments, and the assembly of this network involves actin regulators such as RhoA and the phosphate loop ATPase Nubp1 (Pan et al., 2007; Ioannou et al., 2013). The docking of the basal bodies modifies the formation of the apical actin network, and defects that impair docking are often associated with a thinner cortical actin network (Park et al., 2006; Ioannou et al., 2013). A complex array of planar polarisation events accompanies the process of basal body docking, including those that determine their distance relative to their neighbours (spacing), their positioning relative to the surface area of the plasma membrane (translational polarity), and their tilting and orientation relative to external cues such as fluid flow (rotational polarity) (Mitchell et al., 2007; Werner and Mitchell, 2012). Basal bodies in mouse multiciliated ependymal cells move, mediated by an actin- and non-muscle myosin II-dependent mechanism, to the anterior side of the apical cell membrane (translational polarity) (Hirota et al., 2010). Two pools of cortical actin filaments have been described in *Xenopus*: the apical actin network (at the plane of the basal bodies) and the subapical network (at the plane of the striated rootlets) (Werner et al., 2011). Treatment with a low dose of cytochalasin D, which specifically inhibits the formation of the subapical actin network, leads to defects in basal body spacing and rotational polarity and to subsequent impairment of directional and metachronal ciliary beating and, thereby, to defects in the generation of fluid flow (Werner et al., 2011).

Components of the planar cell polarity (PCP) pathway are important for basal body docking and planar polarisation (Park et al., 2006, 2008; Mitchell et al., 2009). Specifically, Dishevelled interacts with Inturned to control the activation and localisation of the small GTPase Rho at the basal bodies, leading to proper apical docking and polarisation of basal bodies and to Rho-mediated actin assembly (Park et al., 2006, 2008). Basal body migration and docking in MCCs are actin cytoskeleton-dependent steps during ciliogenesis. Rho GTPases are known to be key regulators of the actin cytoskeleton (Hall, 1998). However, the orchestration of the steps and the signalling events leading to changes in actin polymerisation are only incompletely understood.

In ciliogenesis, a role for the Rho family GTPase Rac1 in the positioning of the cilium on the posterior cell surface in mouse ventral node cells has been postulated (Hashimoto et al., 2010), and in Lowe syndrome, a deficiency of Rac1 activity is associated with abnormal primary cilia formation (Madhivanan et al., 2012), but the exact function of Rac1 in these contexts remains unclear. The ELMO-DOCK1 (formerly DOCK180) complex serves as a bipartite guanine nucleotide exchange factor for Rac1 (Brugnera et al., 2002). Several studies have shown the essential function of ELMO1-DOCK1 in remodelling the actin cytoskeleton and controlling cell migration during multiple processes, including engulfment of apoptotic cells, phagocytosis, tumour invasion, myoblast fusion and angiogenesis (Gumienny et al., 2001; Jarzynka et al., 2007; Park et al., 2007; Moore et al., 2007; Elliott et al., 2010;

[1]Renal Division, University Hospital Freiburg, Freiburg 79106, Germany. [2]Department of General Pediatrics, University Children's Hospital Münster, Münster 48149, Germany. [3]Department of Anatomy and Cell Biology, University of Freiburg, Freiburg 79104, Germany. [4]BIOSS Centre for Biological Signalling Studies, University of Freiburg, Freiburg 79108, Germany. [5]Department of Computer Science, University of Freiburg, Freiburg 79110, Germany.

*Author for correspondence (albrecht.kramer-zucker@uniklinik-freiburg.de)

Received 6 May 2014; Accepted 5 November 2014

Development (2015) 142, 174-184 doi:10.1242/dev.112250

Epting et al., 2010), although its potential role during ciliogenesis has not yet been reported. ELMO members interact with ERM proteins (Ezrin, Radixin and Moesin), implying a possible crosstalk between ERMs and ELMO-DOCK1 in coordinating the actin cytoskeleton via Rac1 (Grimsley et al., 2006). ERMs belong to an evolutionarily conserved family of proteins that link membrane-associated proteins to the apical actin network (McClatchey, 2014). Structurally, ERMs consist of an N-terminal FERM (4.1 protein, ERM) domain, which interacts with components at the plasma membrane, and a C-terminal actin-binding domain (Turunen et al., 1994). Interaction of the N-terminal domain with the C-terminus keeps ERMs in an inactive state (Gary and Bretscher, 1995). Phosphorylation of a highly conserved threonine residue unfolds and activates ERMs, which is followed by their translocation to the cell surface (Fievet et al., 2004). Among the ERMs, Ezrin displays a restricted expression pattern, and is found almost exclusively in polarised epithelial cells (Berryman et al., 1993). Ezrin-deficient mice revealed that Ezrin is required for normal intestinal villus formation, underlining the fundamental role of this adaptor component in organising the apical actin network of polarised cells (Saotome et al., 2004). Ezrin localises to the apical membrane and basal bodies of mouse tracheal epithelium, and this localisation requires expression of the ciliogenic transcription factor Foxj1 (Huang et al., 2003; Gomperts et al., 2004).

We now demonstrate that Ezrin, ELMO-DOCK1 and its downstream effector Rac1 cooperate and function as a module during the highly coordinated processes of ciliary basal body targeting and docking to the apical membrane. Depletion of any of these components leads to defects in basal body docking and spacing, and ultimately to defects in ciliary function.

RESULTS

ELMO directs ciliary basal bodies to the apical surface in zebrafish and *Xenopus*

Since the function of Rac1 and its upstream regulators during ciliogenesis remains incompletely understood, we determined the localisation of the Rac1 regulator ELMO1 in human respiratory epithelial cells from healthy persons. Colabelling of ELMO1 with either CEP164, a marker for the mother centriole in monociliated cells (Graser et al., 2007), or acetylated Tubulin, a marker for the ciliary axoneme, revealed specific ELMO1 expression at the basal bodies and along the ciliary axonemes in human respiratory epithelial cells (Fig. 1A-E; supplementary material Fig. S1A-E). Moreover, we analysed the localisation of ELMO1-DOCK1 in non-motile cilia of polarised Madin–Darby canine kidney cells (MDCKs) (supplementary material Fig. S1G,H and Fig. S2). Immunostaining revealed a specific staining pattern for ELMO1 as well as for DOCK1 at the base of the cilium in MDCKs. Co-immunostainings with Cep164 confirmed that ELMO1 was localised exclusively at the mother centriole, whereas DOCK1 localised to both mother and daughter centrioles.

Based on the specific ciliary expression of ELMO1 and DOCK1 in primary non-motile cilia of MDCKs and in motile cilia of human respiratory epithelial cells, we investigated the potential role of the Rac1 activator complex ELMO-DOCK1 during ciliogenesis, using the vertebrate model organisms zebrafish and *Xenopus laevis*. Sections of zebrafish embryos at 36 h post fertilisation (hpf) subject to whole-mount *in situ* hybridisation (WISH) for *elmo1* and *cadherin 17* revealed *elmo1* expression in the pronephric tubule (Fig. 1F). Since there is no working ELMO1 antibody for immunofluorescence, we immunostained for DOCK1 as a surrogate: in 48 hpf *Tg(actb2:Mmu.Arl13b-GFP)* zebrafish embryos (Borovina et al., 2010), Dock1 is localised on the base of the cilia, the presumptive basal bodies, in pronephric tubules and otic vesicles (Fig. 1G-I; supplementary material Fig. S3B-B″). Morpholino oligonucleotide (MO)-mediated knockdown of Elmo1 or Dock1 led to pronephric cyst formation and left-right asymmetry defects at 48 hpf (Fig. 1J-L; supplementary material Fig. S4A) and to shortened cilia in the pronephric tubule of 24 hpf embryos (supplementary material Fig. S4B). These defects are similar to the phenotypic changes observed in mutant zebrafish lines with defective ciliogenesis (Kramer-Zucker et al., 2005), implicating a link between ELMO1-DOCK1 and cilia function. Co-injection of *elmo1* mRNA partially prevented the pronephric cyst formation of *elmo1* morphants, confirming MO specificity (Fig. 1L). Transmission electron microscopy (TEM) studies revealed defective basal body transport to the apical membrane in *elmo1* and *dock1* morphants (Fig. 1M-O′; supplementary material Fig. S4C).

The population of tubular epithelial cells in the zebrafish pronephros consists of monociliated and multiciliated cells (Liu et al., 2007). To confirm the role of ELMO in MCCs, we took advantage of a second animal model, *X. laevis*, since the epidermis of *Xenopus* embryos contains isolated MCCs with motile cilia that are easily accessible for high-resolution imaging (Werner and Mitchell, 2012). *Xenopus* has two ELMO homologues, ELMO1 and ELMO2, which share 70% identity. Both homologues were expressed similarly, including in ciliated tissues (Fig. 2A-F; supplementary material Fig. S5C). The *dock1* mRNA expression pattern partially overlapped with that of *elmo1* and *elmo2* (supplementary material Fig. S5A-C). MOs targeting *elmo1* or *elmo2* (supplementary material Fig. S6A-C) did not have a significant effect when injected separately. However, combined ELMO1 and ELMO2 knockdown in the medium dose range (each 4 ng) caused defects in the apical migration and membrane attachment of basal bodies, as labelled with Centrin-RFP (Park et al., 2008), and the formation of intracellular polymerised acetylated α-Tubulin-positive structures (Fig. 2G,H; supplementary material Fig. S6D,E). Injection of lower doses of *elmo1* and *elmo2* MOs (each 2 ng) resulted in partial basal body docking, but the regular spacing of the basal bodies was impaired, causing basal bodies to be attached to each other like ‘beads on a string’ or to form groups (Fig. 2I-J; supplementary material Fig. S7).

In summary, these results show that ELMO proteins are expressed in ciliated organs in zebrafish and *Xenopus*. The loss-of-function studies reveal that the ELMO-DOCK1 complex is required for specific aspects of cilia formation, i.e. for coordinated basal body docking and spacing across the apical cell membrane.

Ezrin interacts with ELMO and is required for proper ciliogenesis in zebrafish and *Xenopus*

Ezrin is localised on ciliary basal bodies in MCCs (Gomperts et al., 2004). Moreover, Ezrin, similar to other ERMs, physically interacts with members of the ELMO family (Grimsley et al., 2006). First, we studied the expression of Ezrin using human respiratory epithelial cells from controls. Colabelling of Ezrin with α/β-Tubulin revealed specific Ezrin expression at the assumed site of the basal bodies in human respiratory epithelial cells (Fig. 3A-D; supplementary material Fig. S1F). Next, we analysed the expression and function of Ezrin during zebrafish embryogenesis. In zebrafish, two related Ezrin genes exist, termed *ezrin a* and *ezrin b*. WISH identified a tissue-specific expression pattern only for *ezrin b* (supplementary material Fig. S8A-G), which is hereafter referred to as *ezrin*. At larval stages, *ezrin* expression was detected in ciliated tissues, including the olfactory placode/pit, the lining of the brain ventricles, the otic vesicle and throughout the pronephric tubule.

Development (2015) 142, 174-184 doi:10.1242/dev.112250

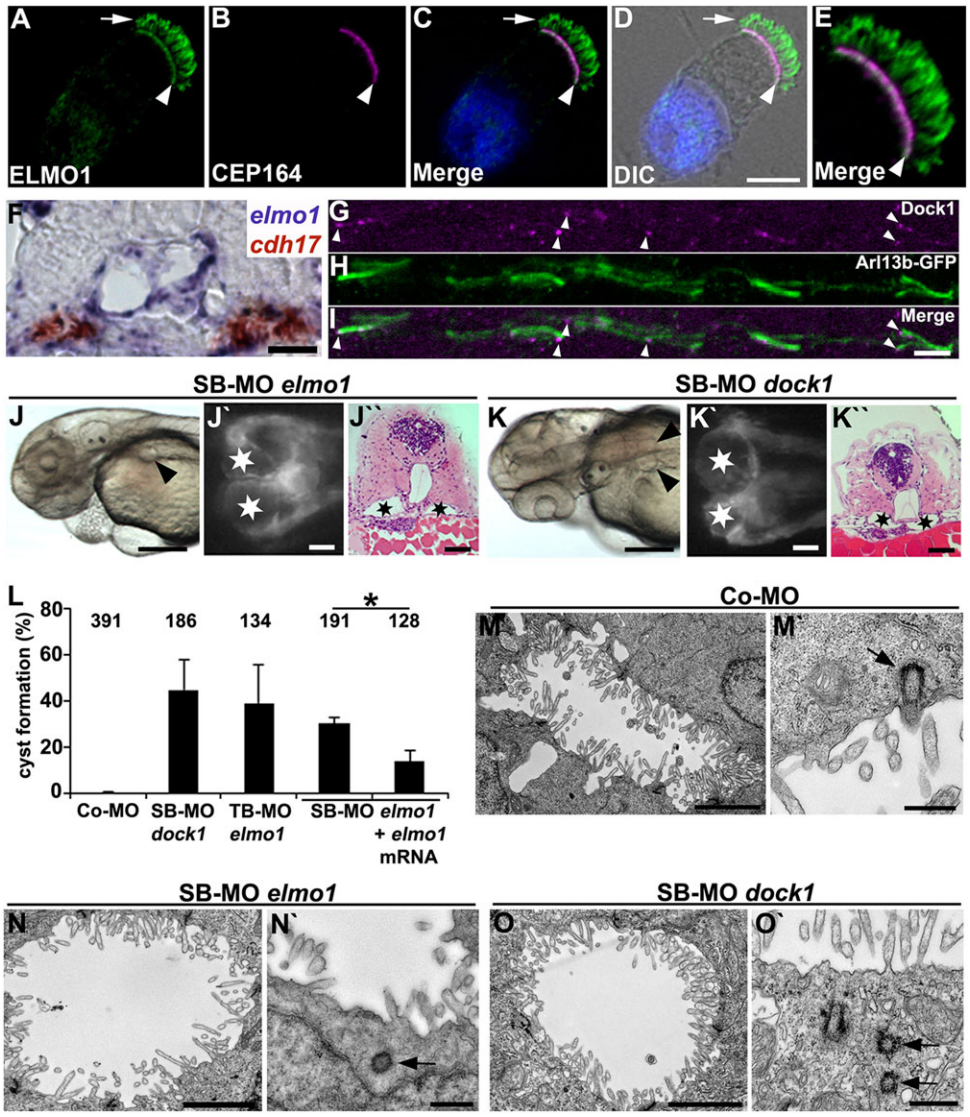

Fig. 1. ELMO1 and DOCK1 show expression in cilia in human and zebrafish and are required for ciliogenesis in zebrafish. (A-E) Human respiratory epithelial cells from healthy controls were double labelled with antibodies against ELMO1 (green) and CEP164 (magenta). ELMO1 localises along the ciliary axonemes (arrow) and the basal bodies (arrowhead). The nucleus is stained with Hoechst 33342 (blue). (F) Transverse section of a 24 hpf zebrafish embryo reveals that *elmo1* mRNA expression (blue) partially colocalises with *cadherin 17* (*cdh17*) mRNA (red) in the pronephric tubule. (G-I) Dock1 is expressed at the base of the cilium (arrowheads) and ciliary axonemes (green fluorescence of Arl13b-GFP) in 48 hpf *Tg(actb2:Mmu.Arl13b-GFP)* zebrafish embryos. (J-K″) Expression silencing of *elmo1* (J-J″) and *dock1* (K-K″) using SB-MO *elmo1* (2 ng) and SB-MO *dock1* (2 ng), respectively, resulted in pronephric cyst formation (arrowheads and stars), as shown in a bright-field lateral view with anterior to the left (J,K), a dorsal view with anterior to the left of a *Tg(wt1b:EGFP)* embryo (J′,K′), and in a transverse section (J″,K″) of 48 hpf embryos. (L) Quantification of pronephric cyst formation in 48 hpf zebrafish embryos injected with Co-MO, SB-MO *dock1*, TB-MO *elmo1* and SB-MO *elmo1* (each 2 ng) or SB-MO *elmo1* (2 ng) + *elmo1* mRNA (20 pg). There was significant prevention of cyst formation upon co-injection of *elmo1* mRNA (*$P \leq 0.05$). The number of individual embryos analysed is indicated above each bar. (M-O′) Analysis of electron micrographs revealed basal body docking defects (arrows) in 48 hpf zebrafish embryos injected with SB-MO *elmo1* (2 ng) (N,N′) or SB-MO *dock1* (2 ng) (O,O′) as compared with Co-MO (2 ng) (M,M′). Scale bars: 10 µm in D; 20 µm in F,J′,K′; 100 µm in I; 50 µm in J,K,J″,K″; 2 µm in M,N,O; 0.5 µm in M′,N′,O′.

Immunostaining localised Ezrin to the base of the cilia in pronephric tubular cells and inner ear cells of 48 hpf *Tg(actb2:Mmu.Arl13b-GFP)* zebrafish embryos (Fig. 3E-G; supplementary material Fig. S3C-C″).

To investigate the role of Ezrin in ciliary function we used an MO that blocks the translation of *ezrin* (Link et al., 2006). Downregulation of Ezrin led to prominent hydrocephalus and pronephric cyst formation in zebrafish embryos (Fig. 3H-J). Moreover, quantification of cilia length in the pronephric tubule revealed significantly shortened cilia in *ezrin* morphants compared with the control at 24 hpf (supplementary material Fig. S4B). Co-injection of *ezrin* mRNA together with MO partially prevented pronephric cyst formation, confirming MO specificity (Fig. 3J; supplementary material Fig. S8H). Examination of the anterior pronephric tubular segments in 48 hpf *ezrin* morphants by TEM revealed defective microvillus formation, and showed that multiple basal bodies did not attach to the apical membrane and that ciliary axoneme formation was impaired (Fig. 3K,K′; supplementary material Fig. S4C). The significant reduction of microvilli (Fig. 3K) supports MO specificity, since it is consistent with the reported role of Ezrin during microvillus formation (Berryman et al., 1993; Crepaldi et al., 1997).

Development (2015) 142, 174-184 doi:10.1242/dev.112250

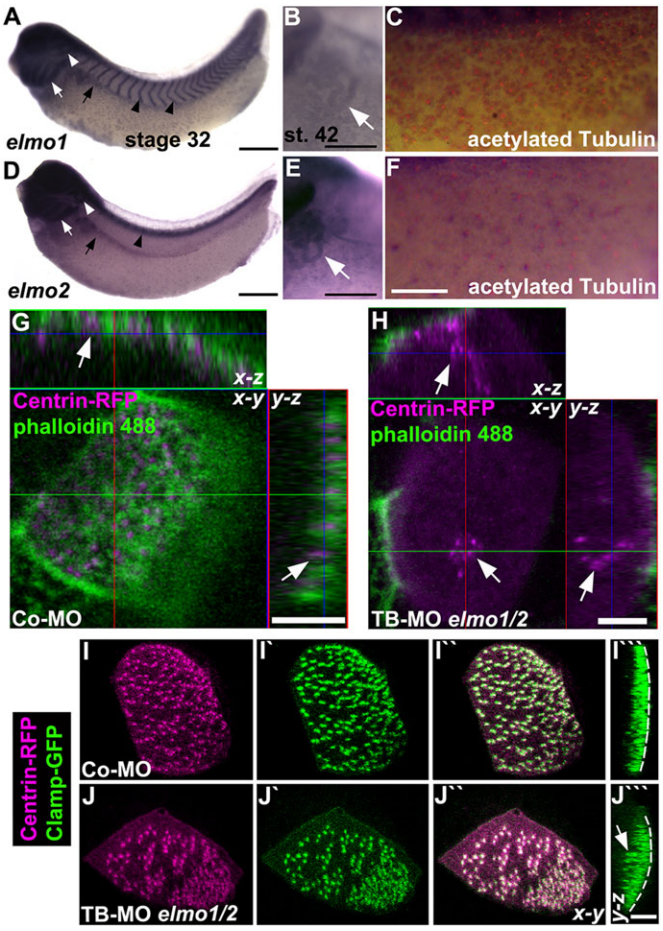

Fig. 2. ELMO1 and ELMO2 are expressed in ciliated organs and are required for ciliogenesis in *Xenopus*. (A-F) Expression of *elmo1* (A-C) and *elmo2* (D-F) in the head, branchial arches (white arrow in A,D), otic vesicle (white arrowhead), pronephric kidney (black arrow), throughout the epidermis at stage 32, and in the pronephric tubules (white arrow in B,E) at stage 42 of *Xenopus* development. In addition, *elmo1* is expressed in the intersomitic vessels and *elmo2* in the spinal cord at stage 32 (black arrowheads). Expression of *elmo1* and *elmo2* colocalised with acetylated Tubulin marking cilia at stage 32 (C,F; see also supplementary material Fig. S5C). (G,H) *Xenopus* embryos (stage 32) injected with TB-MO *elmo1* and TB-MO *elmo2* (each 4 ng) and *centrin-RFP* mRNA colabelled with phalloidin 488 (for F-actin) revealed impaired migration and docking of basal bodies (arrows) to the apical membrane (H) as compared with embryos injected with Co-MO (8 ng) (G). (I-J‴) Injection of *Xenopus* embryos (stage 32) with a lower dose of the TB-MOs (each 2 ng) together with *centrin-RFP* and *clamp-GFP* mRNAs revealed partial basal body docking (arrows) and irregular basal body spacing (I-J‴) compared with proper apically docked and evenly distributed basal bodies in embryos injected with Co-MO (4 ng) (I-I‴). Dashed line indicates the apical surface. Scale bars: 500 µm in A,D; 250 µm in B,E; 2 mm in F; 5 µm in G,H,J‴.

To uncover a potential genetic interaction between *elmo1* and *ezrin* during ciliogenesis in zebrafish, we examined whether the cystic phenotype of *elmo1* or *ezrin* morphants could be prevented by *ezrin* or *elmo1* mRNA, respectively. Indeed, Ezrin or Elmo1 overexpression ameliorated the defects caused by *elmo1* or *ezrin* depletion, respectively, suggesting that both proteins act in the same pathway that coordinates basal body migration and docking in zebrafish (Fig. 3L).

In *Xenopus*, *ezrin* transcripts were expressed in ciliated epithelial cells, including the otic vesicle, cloaca, pronephros and throughout the epidermis at stage 32 of development (supplementary material Fig. S5C and Fig. S8I). Downregulation of Ezrin using a translation-blocking MO (8 ng) (supplementary material Fig. S8J), led to polymerised acetylated α-Tubulin-positive structures within the cytoplasm that did not project to the outside of the cell like normal ciliary axonemes (Fig. 4A,B; supplementary material Fig. S6D). Strikingly, in *ezrin* morphants the basal bodies clustered in the cytoplasm close to the cell centre instead of being transported to the apical membrane and distributed uniformly along the cell surface (Fig. 4C-D‴; supplementary material Fig. S6E). Furthermore, the apical actin network of the MO-affected epidermal cells appeared to be thinner than that of controls, with focal points of actin accumulation at the apical membrane directly above the basal body cluster (Fig. 4D-D″ and Fig. 5A-A‴). TEM confirmed that the basal bodies accumulated at some distance to the apical cell membrane in *ezrin* morphants (Fig. 5C,F). Some ciliary axonemes formed within the cytoplasm in *ezrin* morphants, revealing an ultrastructure identical to the properly elongated axonemes of the controls (Fig. 5C′,C″,E,G). Injection of lower doses of *ezrin* MO (2 and 4 ng) led to a phenotype whereby basal body docking and axoneme formation partially occurred, but spacing of the basal bodies was impaired (Fig. 4E-F‴; supplementary material Fig. S7).

Collectively, these results identify a novel role for ELMO and Ezrin in guiding the maturing basal bodies to the cell surface, in their docking, and in their correct spacing underneath the apical membrane in MCCs.

The ELMO-DOCK1 downstream effector Rac1 is important for basal body docking and spacing

Rac1 is the major downstream effector of ELMO-DOCK1 (Brugnera et al., 2002). In zebrafish there are two related *rac1* genes: *rac1* and *rac1l*. Whereas depletion of *rac1* resulted in minor pronephric cyst formation, depletion of *rac1l* caused prominent pronephric cyst formation (Fig. 6A-C; supplementary material Fig. S9A). Simultaneous knockdown of both proteins caused shortened cilia in the pronephric tubule at 24 hpf (supplementary material Fig. S4B). Co-injection of *rac1l* mRNA partially prevented the pronephric cyst formation of *rac1l* morphants, confirming specificity of the MO (Fig. 6C). In addition, depletion of *rac1* and/or *rac1l* led to striking defects of cardiac looping in zebrafish embryos at 48 hpf, suggesting an essential role of these gene products during the establishment of normal left-right asymmetry (Fig. 6D). TEM studies of *rac1*/*rac1l* double-morphant zebrafish revealed a transport defect and an abnormal accumulation of basal bodies in the cytoplasm at 48 hpf (Fig. 6E-E″; supplementary material Fig. S4C). Consistent with the observed abnormalities in zebrafish, MO depletion of Rac1 during *Xenopus* epidermis development resulted in irregular basal body docking and spacing at the apical membrane (Fig. 6F-H‴; supplementary material Fig. S7).

Rac1 controls ERM phosphorylation during ciliogenesis

During T-cell activation, Rac1 inactivates ERMs in T-lymphocytes, and this results in relaxation of the cortical actin cytoskeleton from the plasma membrane, and leads to the formation of the immunological synapse (Faure et al., 2004; Cernuda-Morollon et al., 2010). To investigate whether Rac1 regulates ERMs during ciliogenesis in vertebrates, we isolated pronephric tubules of 24 hpf zebrafish embryos depleted of *rac1*/*rac1l*, *elmo1* or *dock1* and determined the phosphorylation level of ERMs by immunoblotting. Increased phospho-ERM levels were observed in all three conditions (Fig. 7A), as well as after Rac1 or Rac1l single knockdown (supplementary material Fig. S9A). Reciprocally, overexpression of

Development (2015) 142, 174-184 doi:10.1242/dev.112250

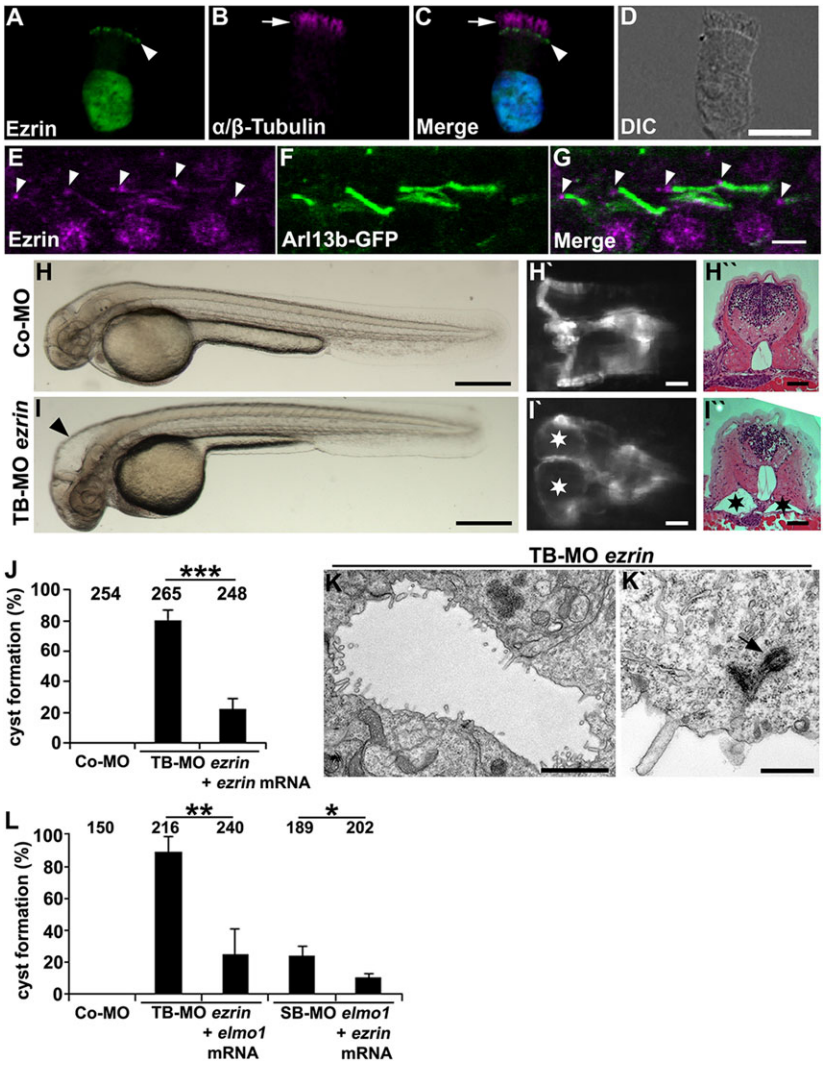

Fig. 3. Ezrin shows expression in cilia and is required for ciliogenesis in zebrafish. (A-D) Human respiratory epithelial cells from healthy controls were double labelled with antibodies directed against Ezrin (green) and the ciliary axoneme marker α/β-Tubulin (magenta) (arrow). Ezrin localisation is restricted to the putative basal bodies (arrowhead) and the nucleus. The nucleus is stained with Hoechst 33342 (blue). (E-G) Ezrin is expressed at the basal bodies (arrowheads) and the ciliary axonemes in 48 hpf *Tg(actb2:Mmu.Arl13b-GFP)* zebrafish embryos. (H-I″) Expression silencing of *ezrin* (I-I″) using TB-MO *ezrin* (2 ng) results in hydrocephalus (arrowhead in I) and pronephric cyst formation (stars in I′ and I″) as compared with zebrafish embryos injected with Co-MO (2 ng) (H-H″), shown in a bright-field lateral view with anterior to the left (H,I), a dorsal view with anterior to the left of a *Tg(wt1b:EGFP)* embryo (H′,I′), and by a histological transverse section (H″,I″) of 48 hpf embryos. (J) Quantification of pronephric cyst formation in 48 hpf zebrafish embryos after injection with TB-MO *ezrin* (2 ng) or TB-MO *ezrin* (2 ng)+ *ezrin* mRNA (20 pg), as compared with Co-MO (2 ng). There is significant prevention of cyst formation upon co-injection of *ezrin* mRNA (***P<0.001). (K,K′) TEM analysis revealed reduced microvilli formation and basal body docking defects in TB-MO *ezrin* (2 ng) morphants at 48 hpf. Arrow indicates prospective basal body not properly docked. (L) Quantification of pronephric cyst formation in 48 hpf zebrafish embryos injected with Co-MO (2 ng), TB-MO *ezrin* (2 ng), TB-MO *ezrin* (2 ng)+ *elmo1* mRNA (20 pg), SB-MO *elmo1* (2 ng) or SB-MO *elmo1* (2 ng)+ *ezrin* mRNA (20 pg) (*P=0.03; **P=0.006). (J,L) The number of individual embryos analysed is indicated above each bar. Scale bars: 10 µm in D; 5 µm in G; 100 µm in H,I; 50 µm in H′, H″,I′,I″; 2 µm in K; 0.5 µm in K′.

Elmo1 or Rac1l resulted in significantly decreased phospho-ERM levels in zebrafish (Fig. 7B).

To determine the function of Ezrin in the zebrafish pronephric tubule, wild-type and mutant forms of zebrafish Ezrin, including the phosphorylation-deficient Ezrin(T564A) mutation and the phosphorylation mimetic mutant Ezrin(T564D) corresponding to human Ezrin threonine 567 (Gautreau et al., 2000), were targeted to the zebrafish pronephros using a transient transgenesis approach (Kikuta and Kawakami, 2009). The *cadherin 17* promoter-driven expression of both mutant forms caused cyst formation on the left- or right-hand side of the pronephric glomerulus, depending on which side the motile cilia bearing MCCs in the mid-portion of the pronephric tubule were most affected (Fig. 7C-F). The majority of MCCs are located in this mid-tubular segment, creating the fluid flow within the pronephric tubule that is necessary for normal pronephric development (Kramer-Zucker et al., 2005; Liu et al., 2007). Moreover, injection of mRNA of either the phosphorylation-deficient *ezrin(T564A)* mutation or the phosphorylation mimetic *ezrin(T564D)* resulted in significantly shortened cilia in the pronephric tubule of 24 hpf zebrafish embryos (supplementary material Fig. S9B-D).

To further confirm a potential role for the ELMO-DOCK1-Rac1 complex in regulating Ezrin phosphorylation levels, we next examined whether overexpression of the phosphorylation-deficient Ezrin(T564A) mutation might prevent the formation of pronephric cysts in Elmo1-, Dock1- or Rac1/Rac1l-deficient zebrafish embryos. Indeed, we were able to show that overexpression of mRNA encoding the phosphorylation-deficient Ezrin(T564A) mutation significantly reduced pronephric cyst formation in all three experimental settings performed at 2 dpf (Fig. 7G).

Taken together, these results indicate that Rac1 plays an essential role during ciliogenesis in vertebrates by acting downstream of ELMO-DOCK1, where it induces Ezrin dephosphorylation.

DISCUSSION

Motile cilia play a central role in embryonic development and human disease. Using two *in vivo* models, zebrafish and *Xenopus*, we identified the protein module encompassing Ezrin, ELMO-DOCK1 and Rac1, as a crucial component for cilia biogenesis and function in MCCs.

ELMO1 localises to the basal bodies in both monociliated and multiciliated cells. Cep164, as a marker of the mother basal body in primary cilia, was reported to localise to all basal bodies in MCCs (Lau et al., 2012). Our findings show a colocalisation of ELMO1 with Cep164 in both cell types (Fig. 1A-E; supplementary material Fig. S2C). In addition, in MDCKs ELMO1 localises to the mother centriole exclusively, whereas DOCK1 was seen at the mother and the daughter centriole. This significant distinction has to be explored in future studies. In non-dividing multiciliated respiratory epithelial cells there is no daughter centriole attached

Development (2015) 142, 174-184 doi:10.1242/dev.112250

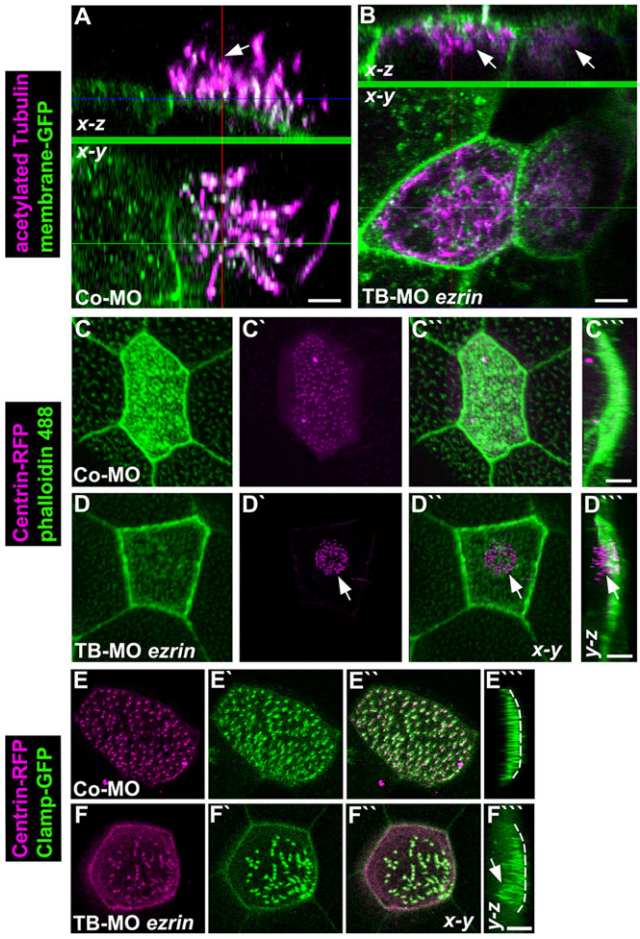

Fig. 4. Ezrin is required for ciliogenesis in *Xenopus*. (A,B) In *Xenopus* embryos (stage 32) injected with Co-MO (8 ng) the cell membrane was highlighted by overexpression of membrane-GFP. Immunostaining for acetylated Tubulin showed the ciliary axonemes protruding to the outside of the cell (A, arrow), whereas in embryos injected with TB-MO *ezrin* (8 ng) the acetylated α-Tubulin-positive structures mainly formed inside the cell (B, arrows). (C-D‴) Basal bodies marked by overexpression of Centrin-RFP aligned properly at the apical cell membrane labelled with phalloidin 488 in *Xenopus* embryos (stage 32) injected with Co-MO (8 ng) (C-C‴), in contrast to the failed migration and docking of basal bodies (arrows) in embryos injected with TB-MO *ezrin* (8 ng) (D-D‴). (E-F‴) Injection of a lower dose of TB-MO *ezrin* (4 ng) together with *centrin-RFP* and *clamp-GFP* mRNA (F-F‴) revealed partial basal body docking (arrow) and irregular basal body spacing compared with proper apically docked and evenly distributed basal bodies in embryos (stage 32) injected with Co-MO (4 ng) (E-E‴). Dashed white line indicates the apical surface. Scale bars: 5 µm.

to the basal body, in contrast to differentiating and dividing respiratory epithelial cells exhibiting primary monocilia (Sorokin, 1968; Dawe et al., 2007; Nigg and Raff, 2009). Cep164 has been implicated in the recruitment of Rab8 and docking of vesicles at the mother centriole to initiate the formation of the primary cilium (Schmidt et al., 2012). Cep164 function in MCCs has not been clearly defined as yet, but basal body docking to ciliary vesicles and migration to the apical cell membrane are conceivable (Sorokin, 1968; Park et al., 2008). Ezrin also localises to the putative basal body in MCCs of the human respiratory epithelium (Fig. 3A-D), very likely together with ELMO1; furthermore, ELMO1 resides in part of the ciliary axoneme (supplementary material Fig. S1A-D). This underlines the role of Ezrin and ELMO1 in ciliogenesis that we have described here.

Depletion of Ezrin, ELMO/DOCK1 or Rac1 by MO injection caused characteristic phenotypes with impaired basal body migration and docking. Rac1 is likely to directly affect filament assembly of the apical actin network, a key structural component of ciliogenesis. Recently, it was proposed that during the process of basal body docking a cytoplasmic actin network, controlled by Nubp1, surrounds the migrating basal bodies and modifies the subapical actin network (Ioannou et al., 2013). Depletion of Nubp1 in *Xenopus* abolished the internal actin network and led to failure of basal body migration. We showed that knockdown of Ezrin in *Xenopus* embryos not only impaired centriole/basal body migration, but also decreased overall actin polymerisation at the apical cell membrane (with the exception of the cortical actin ring along the cell-cell junctions) (Fig. 4D and Fig. 5A), similar to the changes reported in *Xenopus inturned* morphants (Park et al., 2006) or in *nubp1* morphants (Ioannou et al., 2013). This supports the concept of actin filaments acting as a guide structure in the apical migration of basal bodies. However, directly above the cluster of centrioles/basal bodies there are actin foci at the prospective site of docking of the basal bodies (Fig. 4D″ and Fig. 5A″). This would imply that docking could be the trigger for the proper assembly of the apical/subapical actin network, with its delicate structure (Werner et al., 2011). Since the mechanism of Nubp1 action remains unclear but seems to be independent of RhoA, it is tempting to speculate that the Nubp1-mediated actin modification might involve the ELMO-Ezrin-Rac1 module.

Furthermore, a low dose of *nubp1* MO allowed docking of basal bodies, but led to their irregular spacing and to disturbance of the subapical actin pool (Ioannou et al., 2013). Similarly, in *Xenopus* embryos, treatment with a low dose of cytochalasin D mainly affected the subapical actin network and caused defects in basal body spacing (Werner et al., 2011), virtually identical to our observations using MOs at low dosage: basal bodies were attached to each other like ‘beads on a string’ or formed groups (Fig. 2J-J″ and Fig. 4F-F″) instead of being distributed equally throughout the apical cell membrane. In terms of basal body distribution, the changes observed in morphants were significantly different for all MOs compared with the control (supplementary material Fig. S7). In addition, it has been shown that inhibition of Rac1 in mouse nodal cells leads to disturbed posterior positioning of the basal body (translational polarity) and to left-right asymmetry defects (Hashimoto et al., 2010). These observations support our notion that the ELMO-Ezrin-Rac1 module is necessary for basal body positioning and spacing.

Upon depletion of Ezrin and impaired apical migration of basal bodies, we observed intracellular axoneme formation by TEM (Fig. 5C-C″,E,G); similar findings are reported in the literature (Tissir et al., 2010; Werner and Mitchell, 2012; Ioannou et al., 2013). Confocal images showed intracellular polymerised acetylated α-Tubulin-positive structures (Fig. 4B). Whether these acetylated α-Tubulin-positive structures represent intracellular axonemes remains an open question, particularly in consideration of recent data showing that apically formed acetylated microtubules are involved in the radial intercalation of MCCs into the outer epithelial layer of the skin in *Xenopus* (Werner et al., 2014). Radial intercalation precedes or coincides with basal body migration and docking. The presence of acetylated α-Tubulin-positive structures in morphant embryos could therefore also reflect a failure to remove these acetylated Tubulin structures that were involved in radial intercalation. Even when basal body migration was disturbed in many cells, we still observed shorter cilia, rather than their absence, in many parts of the zebrafish

Development (2015) 142, 174-184 doi:10.1242/dev.112250

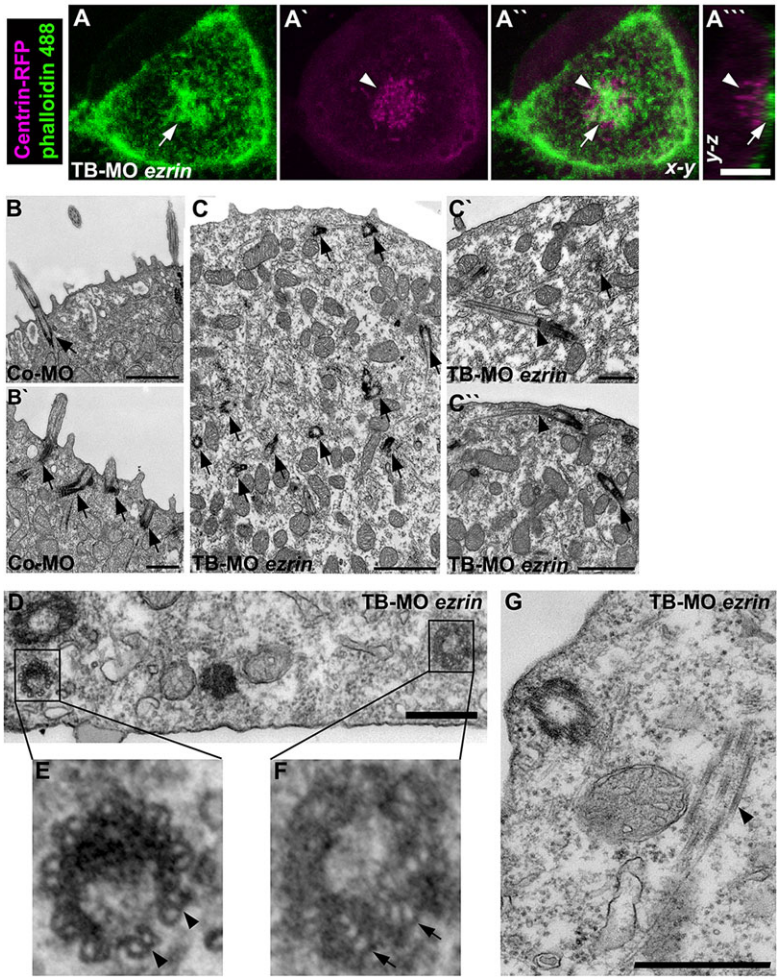

Fig. 5. Ezrin depletion leads to impaired actin remodelling and intracellular ciliary axoneme formation in *Xenopus* MCCs. (A-A‴) Increased actin accumulation (arrows) directly above the cluster of Centrin-RFP-labelled basal bodies (arrowheads) in *Xenopus* embryos (stage 32) injected with TB-MO *ezrin* (8 ng) and stained with phalloidin 488. (B-C″) TEM analysis revealed basal body migration and docking defects (arrows) and intracellular axoneme formation (arrowheads) in *Xenopus* embryos (stage 32) injected with TB-MO *ezrin* (8 ng) (C-C″) as compared with proper apically docked basal bodies (arrows) of Co-MO (8 ng) morphants (B,B′). (D-G) TEM analysis revealed that *Xenopus* embryos (stage 32) injected with TB-MO *ezrin* (8 ng) exhibit a normal ultrastructure of intracellular axonemes with nine outer microtubule doublets and two central microtubule doublets (arrowheads in E,G) and basal bodies with nine peripheral microtubule triplets (arrows in F). Scale bars: 5 µm in A‴; 1 µm in B, C,C″; 0.5 µm in B′,C′,D,G.

pronephric tubules (supplementary material Fig. S4B). Since there are monociliated and multiciliated pronephric tubule cells (Liu et al., 2007), one possible explanation is that monociliated cells are less affected by defective ELMO/Ezrin signalling and therefore still form a cilium. Consistent with this possibility, *Xenopus vangl2* morphants are characterised by a reduced number of cilia in skin cells (Mitchell et al., 2009), whereas cilia in the gastrocoel roof plate are reportedly unaffected (Antic et al., 2010; Werner and Mitchell, 2012). In the same way, gastrocoel roof plate cilia are significantly shorter but not missing in *nubp1* morphants (Ioannou et al., 2013).

With respect to the apical actin network, the function of the basal body in the cilium and of the centrosome in the immunological synapse share striking similarities (Griffiths et al., 2010). T-cell receptor signalling initially leads to actin accumulation across the synapse (Ryser et al., 1982). This is followed by actin clearance in the centre of the synapse, forming an outer ring around the synapse, and by migration of the centrosome to the centre of the synapse (Stinchcombe et al., 2006). T-cell receptor signalling also activates Rac1, leading to dephosphorylation of ERMs, which in turn releases the cross-linking between cell membrane and actin filaments and leads to relaxation of the cytoskeleton and to the formation of a stable T-cell–antigen-presenting cell conjugate (Faure et al., 2004; Cernuda-Morollon et al., 2010). In parallel to centriole migration to the centre of the immunological synapse, basal body migration and docking seem to require such regulation of ERM protein activity: we found that Rac1 and its regulators control ERM phosphorylation. Depletion of members of the ELMO-DOCK1-Rac1 module led to an increase in phospho-Ezrin, whereas overexpression led to its decrease (Fig. 7A,B; supplementary material Fig. S9A). The phenotypic effects caused by MO knockdown of ELMO, DOCK1 or Rac1 were reversed by co-injection of the phosphorylation-deficient zebrafish Ezrin(T564A) (corresponding to threonine T567 in human Ezrin). Moreover, the overexpression of either the phosphorylation-deficient Ezrin(T564A) or the phosphorylation-mimetic Ezrin (T564D) caused pronephric cyst formation (Fig. 7C-F). This implies that tight regulation of Ezrin phosphorylation is mandatory to ensure normal embryonic development. Regulated turnover of Ezrin(T567) phosphorylation has been observed in renal epithelial cells; the phosphorylation mimetic Ezrin(T567D) does not allow such a turnover and its overexpression causes aberrant growth of membrane projections in cultured proximal tubule cells (Zhu et al., 2008). Similar findings have been reported in Jeg-3 cells: hyperphosphorylation of Ezrin induced by phosphatase inhibition led to partial mislocalisation of Ezrin; furthermore, the phosphorylation mimetic Ezrin(T567E) mutant mislocalised all over the plasma membrane, whereas the phosphorylation-deficient Ezrin(T567A) mutant was hardly detected at the plasma membrane (Viswanatha et al., 2012). There was also evidence that Ezrin underwent constant C-terminal phosphocycling, i.e. repetitive phosphorylation and dephosphorylation (Viswanatha et al., 2012). Since we were able to show that both mutant forms of Ezrin (T564A and T564D) caused pronephric cyst formation and also reduced ciliary axoneme length in zebrafish pronephros, as in the

Development (2015) 142, 174-184 doi:10.1242/dev.112250

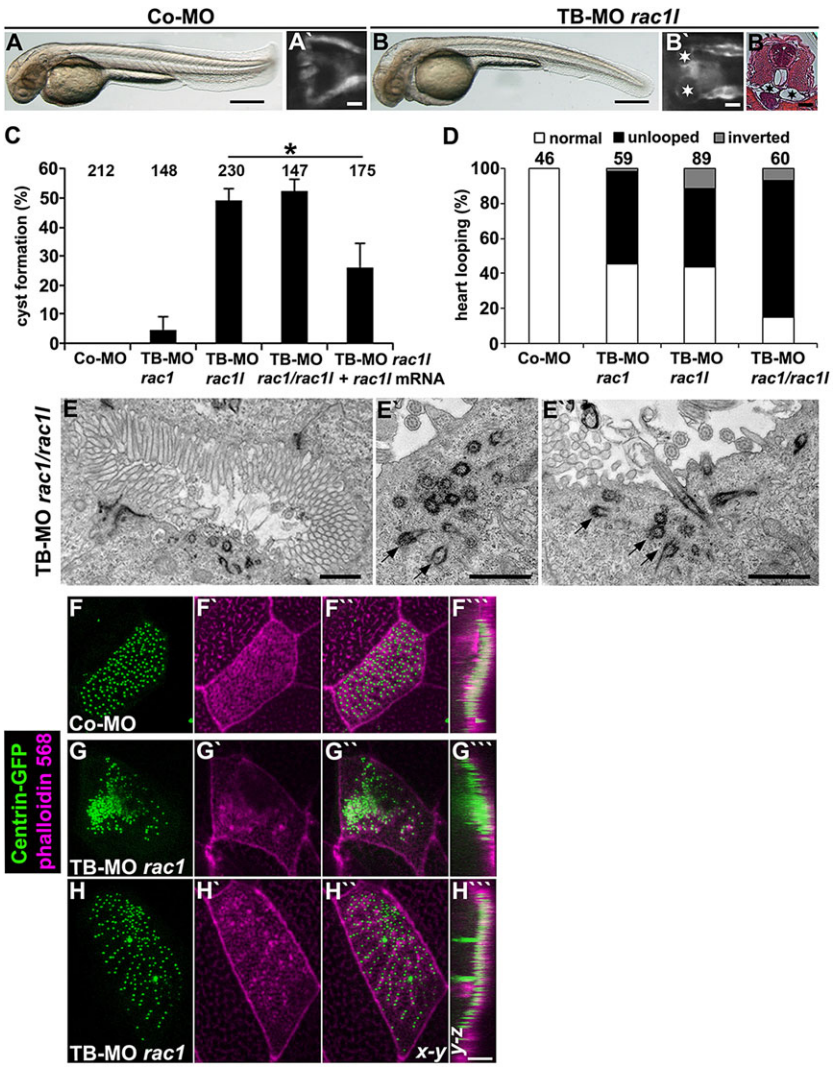

Fig. 6. Rac1 is required for ciliogenesis in zebrafish and *Xenopus*. (A-B″) Expression silencing of Rac1l using TB-MO *rac1l* (0.5 ng) results in pronephric cyst formation (stars in B′ and B″) as compared with Co-MO (0.5 ng) morphants (A′), as shown in a dorsal view with anterior to the left of a *Tg(wt1b:EGFP)* zebrafish embryo (A′,B′) and in a histological transverse section (B″) of a 48 hpf embryo. (A,B) Embryos are shown in bright-field lateral view, with anterior to the left. (C) Quantification of pronephric cyst formation in 48 hpf zebrafish embryos injected with Co-MO (4.5 ng), TB-MO *rac1* (4 ng), TB-MO *rac1l* (0.5 ng), TB-MO *rac1* (4 ng)/*rac1l* (0.5 ng) and TB-MO *rac1l* (0.5 ng)+ *rac1l* mRNA (20 pg). There was significant prevention of cyst formation by co-injection with *rac1l* mRNA (*$P \leq 0.05$). (D) Quantification of laterality defects by *cmlc2 in situ* hybridisation revealed impaired heart looping in 48 hpf zebrafish embryos injected with TB-MO *rac1* (4 ng), TB-MO *rac1l* (0.5 ng), and TB-MO *rac1* (4 ng)/*rac1l* (0.5 ng) compared with Co-MO (4.5 ng). (C,D) The number of individual embryos analysed is indicated above each bar. (E-E″) Analysis of electron micrographs revealed basal body docking defects (arrows in E′,E″) on sections of 48 hpf zebrafish embryos injected with TB-MO *rac1* (4 ng)/*rac1l* (0.5 ng). (F-F‴) *Xenopus* embryos injected with Co-MO (40 ng) and *centrin-GFP* mRNA showed normal basal body docking and basal body distribution at stage 32; embryos were colabelled with phalloidin 568 (magenta). (G-H‴) *Xenopus* embryos (stage 32) injected with TB-MO *rac1* (40 ng) exhibited irregular basal body docking and distribution, 'beads on a string' pattern in H. Scale bars: 100 µm in A,B; 20 µm in A′,B′; 50 µm in B″; 1 µm in E-E″; 5 µm in H‴.

knockdown experiments, this suggests that phosphocycling might be necessary during basal body migration and docking, allowing Ezrin to constantly bind to and release actin filaments.

How does Rac1 influence Ezrin phosphorylation? The increase in threonine phosphorylation of ERM proteins observed after knockdown of the ELMO1-DOCK1-Rac1 complex could reflect a Rac1-dependent inactivation of a constitutively active kinase and/or a Rac1-dependent activation of a serine/threonine phosphatase. According to Parameswaran and Gupta (2013), the phosphatase that inactivates ERM proteins *in vivo* has not yet been identified. In flies, the phosphatase PP1-87B/Sds22 (which is also known as PPP1R7 in mammals) can reverse Moesin phosphorylation (Roubinet et al., 2011). Furthermore, Phosphatase of regenerating liver-3 (PRL-3, also known as PTP4a3) has been shown to be a direct and specific phosphatase for Ezrin(phospho-T567) (Forte et al., 2008). We examined the potential role of PRL-3 in regulating Ezrin phosphorylation downstream of Rac1 in zebrafish. There are two PRL-3 orthologues in zebrafish: Ptp4a3 and Ptp4a3l (ptp4a3, ZFIN, NP_998346, ENSDARG00000039997; ptp4a3l, ZFIN si:ch211-251p5.5, UniProtKB: E7FA22, ENSDARG00000054814). Depletion of Ptp4a3 or Ptp4a3l by MO knockdown did not result in pronephric cyst formation (data not shown). So Ptp4a3 and Ptp4a3l do not seem to be the main phosphatases regulating Ezrin phosphorylation downstream of Rac1 during ciliogenesis in zebrafish. In addition, other potentially relevant phosphorylation sites in different domains of Ezrin have been reported (e.g. Murchie et al., 2014). Thus, the link between Rac1 signalling and the phosphorylation status of ERM proteins remains to be determined and will be the subject of future investigation in our laboratory.

Recently, new gene defects in MCCs of the respiratory epithelium have been identified as causing a distinct mucociliary clearance disorder in humans that is characterised by the reduced generation of multiple motile cilia (RGMC) (Boon et al., 2014; Wallmeier et al., 2014). Individuals show the typical signs of chronic recurrent airway infections, but also hydrocephalus. TEM studies revealed normal microvilli at the apical cell membrane, but a substantial decrease in basal bodies and apical cilia. The responsible genes were identified as *MCIDAS* and *CCNO*, which encode multicilin and cyclin O, respectively, and are implicated in the acentriolar, deuterosome-mediated amplification of centrioles in MCCs, which could be confirmed in *Xenopus*. Since ELMO-DOCK1-Rac1 and Ezrin are potential candidates for RGMC, although with a predominant basal body migration defect, it will be interesting to screen databases of patients with RGMC for defects in these genes.

We present a model for the function of Ezrin and its interactors ELMO and DOCK1 in MCCs (Fig. 8). In conclusion, the Ezrin-ELMO-DOCK1-Rac1 complex represents a newly identified

Development (2015) 142, 174-184 doi:10.1242/dev.112250

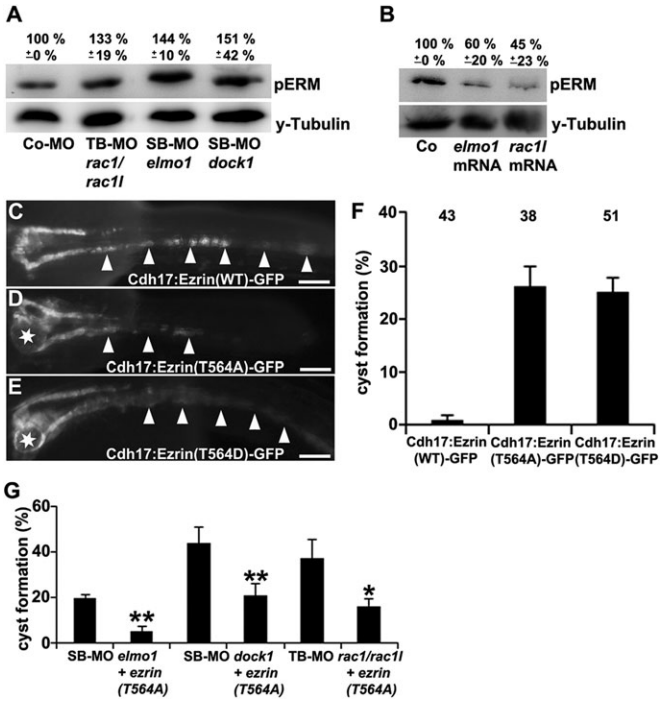

Fig. 7. The ELMO1-DOCK1-Rac1 complex influences ERM phosphorylation and tight control of phospho-Ezrin is required for proper ciliogenesis. (A) Immunoblot of 24 hpf zebrafish lysates showing elevated phospho-Ezrin (pERM) levels in embryos injected with TB-MO *rac1* (4 ng)/*rac1l* (0.5 ng), SB-MO *elmo1* (2 ng) and SB-MO *dock1* (2 ng) as compared with Co-MO (4.5 ng). (B) Immunoblot of 24 hpf zebrafish lysates showing reduced pERM levels in zebrafish embryos injected with *elmo1* mRNA (20 pg) or *rac1l* mRNA (20 pg) as compared with control embryos. Anti-γ-Tubulin immunoblots served as a loading control. Immunoblots represent results from one of three independent experiments with similar results. (C-F) Overexpression of Ezrin by transient transgenesis demonstrates the importance of tight regulation of phosphorylation at threonine 564 for the function of zebrafish Ezrin. *cadherin 17* (*cdh17*) promoter-driven expression of either the nonphosphorylatable T564A mutation or the phosphorylation mimetic mutant T564D caused cyst formation on the side of the pronephros where the MCCs in the mid-portion of the pronephric tubule are most affected. Arrowheads indicate the tubular mid-portion, with the cells expressing mutant Ezrin on the side of the formed cyst. The number of individual embryos analysed is indicated above each bar. (G) Quantification of pronephric cyst formation of 48 hpf zebrafish embryos injected with SB-MO *elmo1* (2 ng) with or without *ezrin(T564A)* mRNA (10 pg) (**P=0.006), SB-MO *dock1* (2 ng) with or without *ezrin(T564A)* mRNA (10 pg) (**P=0.009) or TB-MO *rac1* (4 ng)/*rac1l* (0.5 ng) with or without *ezrin(T564A)* mRNA (10 pg) (*P=0.02). Scale bars: 50 µm.

module that, by influencing the cortical actin web in MCCs, orchestrates ciliary basal body migration, docking and spacing at the apical cell membrane.

MATERIALS AND METHODS

Zebrafish lines and *Xenopus*, embryo maintenance

All animal work has been conducted according to relevant national and international guidelines [Regional council (Regierungspräsidium) Freiburg, reference number 35·9185.64/1.1] (Westerfield, 1995). Zebrafish were maintained and the embryos were staged as previously described (Kimmel et al., 1995). The following strains were used: AB/TL wild type (WT), *Tg(wt1b:EGFP)* (Perner et al., 2007) and *Tg(actb2:Mmu.Arl13b-GFP)* (Borovina et al., 2010). The *Tg(cadherin17-GFP)* line was generated by injection of a Tol2 vector (Kawakami et al., 2004) containing a 4 kb fragment from the zebrafish *cadherin 17* promoter driving the expression of GFP protein. Methods of *X. laevis* maintenance and manipulation were as described (Hoff et al., 2013).

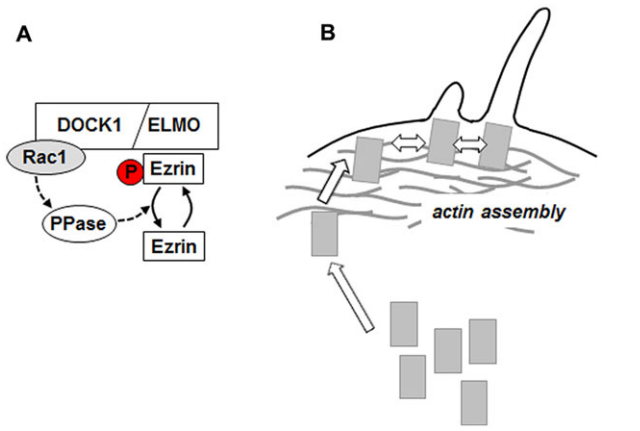

Fig. 8. Model illustrating ELMO-DOCK1-Rac1 and their interaction with Ezrin and the effects on basal body migration and spacing in MCCs. (A) The ELMO-DOCK1 complex localises to the ciliary basal body and acts as bipartite guanine nucleotide exchange factor for Rac1. Rac1 in turn dephosphorylates Ezrin via an unknown phosphatase (PPase). Dephosphorylated Ezrin does not bind to actin filaments, whereas phosphorylated Ezrin serves as a linker between the basal body and actin filaments. (B) Constant turnover of phosphorylated Ezrin regulated by ELMO-DOCK1-Rac1 is necessary to promote basal body migration along actin filaments (arrows) and for basal body docking to the membrane and spacing (double arrows) with assembly of the apical and subapical actin network.

Constructs, mRNAs and MOs

Constructs carrying wild-type and mutant forms of zebrafish Ezrin under the *cadherin 17* promoter [Cdh17:Ezrin(WT)-GFP, Cdh17:Ezrin(T564A)-GFP and Cdh17:Ezrin(T564D)-GFP] were generated and injected as described in the supplementary methods. Synthesis of mRNAs, MO sequences and their injection are described in the supplementary methods. Translation-blocking and splice-blocking MOs are given the prefix TB and SB, respectively.

Antibodies and reagents

The following antibodies were used for immunofluorescence (IF) and immunoblotting (IB): anti-ELMO1 [EB05297, Everest Biotech; human respiratory epithelial cells, 1:150 (IF), 1:500 (IB); MDCKs 1:200 (IF), 1:500 (IB); *Xenopus* 1:1000 (IB)], anti-ELMO2 [EB05305, Everest Biotech; *Xenopus* 1:1000 (IB)], anti-DOCK1 (H-4; sc-13163, Santa Cruz Biotechnology; MDCKs 1:200 (IF, IB); zebrafish 1:50 (IF)], anti-acetylated Tubulin [clone 6-11B-1, Sigma Aldrich; human respiratory epithelial cells 1:10000 (IF); zebrafish and Xenopus 1:500 (IF)], anti-Tubulin [detyrosinated; AB3201, Upstate; MDCKs 1:200 (IF)], anti-γ-Tubulin [clone GTU-88, Sigma Aldrich; zebrafish and *Xenopus* 1:1000 (IB)], α/β-Tubulin [#2148, Cell Signaling; human respiratory epithelial cells 1:300 (IF)], anti-pERM [#3141, Cell Signaling; zebrafish 1:1000 (IB)], anti-oesin [610401, BD Biosciences; human respiratory epithelial cells, 1:100 (IF), 1:500 (IB); MDCKs 1:1000 (IB); zebrafish 1:200 (IF), 1:1000 (IB); *Xenopus* 1:1000 (IB)], anti-Cep164 [provided by Erich Nigg, Basel, Switzerland; MDCKs 1:200 (IF)], anti-Cep164 [AP23475PU-N, Acris Antibodies; human respiratory epithelial cells 1:100 (IF), 1:500 (IB)], anti-Rac1 [clone 23A8, Upstate; zebrafish 1:1000 (IB)], anti-GFP [LS-C144578-100, Biozol; zebrafish 1:200 (IF)]. HRP-conjugated antibodies (DAKO, 1:3000). Cy3-, Cy5- or Alexa Fluor 488/546-labelled secondary antibodies were purchased from Jackson ImmunoResearch and Molecular Probes (Invitrogen), 1:1000 dilution. Alexa Fluor 488/568-phalloidin was purchased from Life Technologies (1:200 dilution) and Hoechst 33342 from Sigma Aldrich, 1:1000 dilution. Details of staining and imaging are provided in the supplementary methods.

Immunoblotting

Zebrafish embryos were lysed in 2× SDS protein sample buffer [0.125 mM Tris-HCl (pH 6.8), 4% SDS, 20% glycerol, 10% β-mercaptoethanol,

Development (2015) 142, 174-184 doi:10.1242/dev.112250

0.004% Bromophenol Blue]. For zebrafish pronephric tubule isolation, 60 control or morphant *Tg(cadherin17-GFP)* embryos were treated with Hank's solution (Westerfield, 1995) containing 0.1 M DTT, 2 mM Na_3VO_4 and protease inhibitors (Roche) for 30 min at room temperature, followed by collagenase digestion [5% collagenase (Sigma-Aldrich) in Hank's solution] for 30 min at room temperature. GFP-fluorescent pronephric tubules were collected and lysed in 2× SDS protein sample buffer. For *Xenopus* protein analysis, embryos were lysed in buffer containing 50 mM Tris (pH 7.6), 1% Triton X-100, 50 mM NaCl, 1 mM EDTA, 2 mM Na_3VO_4 and protease inhibitors (Roche). After centrifugation at 13,000 ***g*** for 5 min, 2× SDS protein sample buffer was added to the supernatant, and the mixture was heated for 5 min at 95°C. Proteins were separated by SDS-PAGE, transferred to PVDF membrane, and incubated with the indicated antibodies and finally with immunoblot detection reagent (Perbio Science).

In situ hybridisation analysis and antisense RNA synthesis

Whole-mount *in situ* hybridisation (WISH) analysis using Digoxigenin- or Fluorescein-labelled probes was performed as described (Epting et al., 2007) using NBT (blue) or INT (red) (Roche) as substrates. Details of staining and imaging are provided in the supplementary methods. Zebrafish antisense RNA was synthesized from *Eco*RI-digested ELMO1-pSPORT1 (EST clone IMAGp998P118966Q; imaGenes) or *Not*I-digested Cadherin17-pCR-BluntII-TOPO [amplified from zebrafish cDNA with specific primers (forward: ATTGATGCCCGTAATCCCGAGC, reverse: ATGCCAAGCC-CAGCGTTGTCTAAG)] plasmid using SP6 RNA polymerase, and from *Eco*RV-digested Ezrin-pExpress-1 (EST clone IRBOp991H0494D; imaGenes) or *Not*I-digested CMLC2-pBluescript II Sk(+) (kindly provided by Wolfgang Driever, Freiburg, Germany) plasmid using T7 RNA polymerase. *Xenopus* antisense RNA was synthesized from *Sma*I-digested ELMO1-pCS111 (EST clone 8547184; Open Biosystems), *Eco*RV-digested ELMO2-pExpress-1 (EST clone 7210931; Open Biosystems), *Not*I-digested DOCK1-pBluescript II Sk(+) (EST clone XL151h21; RIKEN BioResource Center) or *Sal*I-digested Ezrin-pCMV-SPORT6 (EST clone 7011343; Open Biosystems) plasmid using T7 RNA polymerase.

Electron microscopy

Xenopus and zebrafish embryos were fixed and subjected to TEM as detailed in the supplementary methods.

Statistical analysis and quantification

All data represent results from at least one of three independent experiments with similar results. For the quantification of cilia length in the pronephric tubule, cilia were measured in the anterior and the posterior segment of three zebrafish embryos at 24 hpf for each set of conditions. Numbers of embryos used for analysis are indicated in the respective bar chart unless otherwise stated. Data were analysed by Student's *t*-test (two-sided, unpaired); error bars represent s.d. Immunoblot signals were quantified using Gel-Pro Analyzer 6.0, INTAS and normalised to respective loading controls. To quantify the regularity of basal body spacing we developed an image analysis pipeline; the individual steps and associated statistical analysis are explained in detail in the supplementary methods.

Accession numbers

Corresponding GenBank accession numbers for zebrafish cDNAs: *ezrin a* (NM_001020490), *ezrin b* (NM_001030285), *elmo1* (NM_213091), *dock1* (*dock1*) (NM_001110011), *rac1* (NM_199771), *rac1l* (KF273902). For *X. laevis* cDNAs: *ezrin* (NM_001093923), *elmo1* (NM_001090018), *elmo2* (NM_001096183), *rac1* (BC108884).

Acknowledgements

We thank Annette Schmitt, Simone Bräg, Alena Sammarco and Angelina Heer for excellent technical assistance; the Life Imaging Center of the University of Freiburg for use of confocal microscopes and technical support; and members of the Renal Division for helpful discussions.

Competing interests

The authors declare no competing financial interests.

Author contributions

Experiments were designed by D.E., K.S., C.B., N.T.L., S.S.L., H.O., O.R. and A.K.-Z. Experiments were performed by D.E., C.B., S.H., N.T.L., T.Y., L.I. and S.N. Data were interpreted by D.E., K.S., C.B., S.H., T.Y., S.S.L., E.W.K., O.R., G.W. and A.K.-Z. The paper was written by D.E., K.S., E.W.K., O.R., G.W. and A.K.-Z.

Funding

S.S.L., E.W.K., G.W. and A.K.-Z. are supported by the Deutsche Forschungsgemeinschaft (DFG) [KFO 201]. S.S.L. is supported by the Emmy Noether Programme of the DFG. O.R. and G.W. are supported by the Excellence Initiative of the German Federal and State Governments [EXC 294 - BIOSS] and G.W. by the European Community's Seventh Framework Program [grant agreement number 241955, SYSCILIA]. H.O. is supported by the DFG [Om 6/4], by the Interdisziplinäres Zentrum für Klinische Forschung (IZKF) [Om2/009/12] Münster, by the European Community's Seventh Framework Programme [FP7/2009, under grant agreement 241955, SYSCILIA, and BESTCILIA, under grant agreement 305404].

Supplementary material

Supplementary material available online at
http://dev.biologists.org/lookup/suppl/doi:10.1242/dev.112250/-/DC1

References

Antic, D., Stubbs, J. L., Suyama, K., Kintner, C., Scott, M. P. and Axelrod, J. D. (2010). Planar cell polarity enables posterior localization of nodal cilia and left-right axis determination during mouse and Xenopus embryogenesis. *PLoS ONE* **5**, e8999.

Berryman, M., Franck, Z. and Bretscher, A. (1993). Ezrin is concentrated in the apical microvilli of a wide variety of epithelial cells whereas moesin is found primarily in endothelial cells. *J. Cell Sci.* **105**, 1025–1043.

Boisvieux-Ulrich, E., Lainé, M.-C. and Sandoz, D. (1990). Cytochalasin D inhibits basal body migration and ciliary elongation in quail oviduct epithelium. *Cell Tissue Res.* **259**, 443-454.

Boon, M., Wallmeier, J., Ma, L., Loges, N. T., Jaspers, M., Olbrich, H., Dougherty, G. W., Raidt, J., Werner, C., Amirav, I. et al. (2014). MCIDAS mutations result in a mucociliary clearance disorder with reduced generation of multiple motile cilia. *Nat. Commun.* **5**, 4418.

Borovina, A., Superina, S., Voskas, D. and Ciruna, B. (2010). Vangl2 directs the posterior tilting and asymmetric localization of motile primary cilia. *Nat. Cell Biol.* **12**, 407-412.

Brugnera, E., Haney, L., Grimsley, C., Lu, M., Walk, S. F., Tosello-Trampont, A. C., Macara, I. G., Madhani, H., Fink, G. R. and Ravichandran, K. S. (2002). Unconventional Rac-GEF activity is mediated through the Dock180-ELMO complex. *Nat. Cell Biol.* **4**, 574-582.

Cernuda-Morollón, E., Millán, J., Shipman, M., Marelli-Berg, F. M. and Ridley, A. J. (2010). Rac activation by the T-cell receptor inhibits T cell migration. *PLoS ONE* **5**, e12393.

Crepaldi, T., Gautreau, A., Comoglio, P. M., Louvard, D. and Arpin, M. (1997). Ezrin is an effector of hepatocyte growth factor-mediated migration and morphogenesis in epithelial cells. *J. Cell Biol.* **138**, 423-434.

Dawe, H. R., Farr, H. and Gull, K. (2007). Centriole/basal body morphogenesis and migration during ciliogenesis in animal cells. *J. Cell Sci.* **120**, 7-15.

Elliott, M. R., Zheng, S., Park, D., Woodson, R. I., Reardon, M. A., Juncadella, I. J., Kinchen, J. M., Zhang, J., Lysiak, J. J. and Ravichandran, K. S. (2010). Unexpected requirement for ELMO1 in clearance of apoptotic germ cells in vivo. *Nature* **467**, 333-337.

Epting, D., Vorwerk, S., Hageman, A. and Meyer, D. (2007). Expression of rasgef1b in zebrafish. *Gene Expr. Patterns* **7**, 389-395.

Epting, D., Wendik, B., Bennewitz, K., Dietz, C. T., Driever, W. and Kroll, J. (2010). The Rac1 regulator ELMO1 controls vascular morphogenesis in zebrafish. *Circ. Res.* **107**, 45-55.

Faure, S., Salazar-Fontana, L. I., Semichon, M., Tybulewicz, V. L. J., Bismuth, G., Trautmann, A., Germain, R. N. and Delon, J. (2004). ERM proteins regulate cytoskeleton relaxation promoting T cell-APC conjugation. *Nat. Immunol.* **5**, 272-279.

Fievet, B. T., Gautreau, A., Roy, C., Del Maestro, L., Mangeat, P., Louvard, D. and Arpin, M. (2004). Phosphoinositide binding and phosphorylation act sequentially in the activation mechanism of ezrin. *J. Cell Biol.* **164**, 653-659.

Forte, E., Orsatti, L., Talamo, F., Barbato, G., De Francesco, R. and Tomei, L. (2008). Ezrin is a specific and direct target of protein tyrosine phosphatase PRL-3. *Biochim. Biophys. Acta* **1783**, 334-344.

Gary, R. and Bretscher, A. (1995). Ezrin self-association involves binding of an N-terminal domain to a normally masked C-terminal domain that includes the F-actin binding site. *Mol. Biol. Cell* **6**, 1061-1075.

Gautreau, A., Louvard, D. and Arpin, M. (2000). Morphogenic effects of ezrin require a phosphorylation-induced transition from oligomers to monomers at the plasma membrane. *J. Cell Biol.* **150**, 193-204.

Goetz, S. C. and Anderson, K. V. (2010). The primary cilium: a signalling centre during vertebrate development. *Nat. Rev. Genet.* **11**, 331-344.

Development (2015) 142, 174-184 doi:10.1242/dev.112250

Gomperts, B. N., Gong-Cooper, X. and Hackett, B. P. (2004). Foxj1 regulates basal body anchoring to the cytoskeleton of ciliated pulmonary epithelial cells. *J. Cell Sci.* **117**, 1329-1337.
Graser, S., Stierhof, Y.-D., Lavoie, S. B., Gassner, O. S., Lamla, S., Le Clech, M. and Nigg, E. A. (2007). Cep164, a novel centriole appendage protein required for primary cilium formation. *J. Cell Biol.* **179**, 321-330.
Griffiths, G. M., Tsun, A. and Stinchcombe, J. C. (2010). The immunological synapse: a focal point for endocytosis and exocytosis. *J. Cell Biol.* **189**, 399-406.
Grimsley, C. M., Lu, M., Haney, L. B., Kinchen, J. M. and Ravichandran, K. S. (2006). Characterization of a novel interaction between ELMO1 and ERM proteins. *J. Biol. Chem.* **281**, 5928-5937.
Gumienny, T. L., Brugnera, E., Tosello-Trampont, A.-C., Kinchen, J. M., Haney, L. B., Nishiwaki, K., Walk, S. F., Nemergut, M. E., Macara, I. G., Francis, R. et al. (2001). CED-12/ELMO, a novel member of the CrkII/Dock180/Rac pathway, is required for phagocytosis and cell migration. *Cell* **107**, 27-41.
Hall, A. (1998). Rho GTPases and the actin cytoskeleton. *Science* **279**, 509-514.
Hashimoto, M., Shinohara, K., Wang, J., Ikeuchi, S., Yoshiba, S., Meno, C., Nonaka, S., Takada, S., Hatta, K., Wynshaw-Boris, A. et al. (2010). Planar polarization of node cells determines the rotational axis of node cilia. *Nat. Cell Biol.* **12**, 170-176.
Hildebrandt, F., Benzing, T. and Katsanis, N. (2011). Ciliopathies. *N. Engl. J. Med.* **364**, 1533-1543.
Hirota, Y., Meunier, A., Huang, S., Shimozawa, T., Yamada, O., Kida, Y. S., Inoue, M., Ito, T., Kato, H., Sakaguchi, M. et al. (2010). Planar polarity of multiciliated ependymal cells involves the anterior migration of basal bodies regulated by non-muscle myosin II. *Development* **137**, 3037-3046.
Hoff, S., Halbritter, J., Epting, D., Frank, V., Nguyen, T.-M. T., van Reeuwijk, J., Boehlke, C., Schell, C., Yasunaga, T., Helmstädter, M. et al. (2013). ANKS6 is a central component of a nephronophthisis module linking NEK8 to INVS and NPHP3. *Nat. Genet.* **45**, 951-956.
Huang, T., You, Y., Spoor, M. S., Richer, E. J., Kudva, V. V., Paige, R. C., Seiler, M. P., Liebler, J. M., Zabner, J., Plopper, C. G. et al. (2003). Foxj1 is required for apical localization of ezrin in airway epithelial cells. *J. Cell Sci.* **116**, 4935-4945.
Ioannou, A., Santama, N. and Skourides, P. A. (2013). Xenopus laevis nucleotide binding protein 1 (xNubp1) is important for convergent extension movements and controls ciliogenesis via regulation of the actin cytoskeleton. *Dev. Biol.* **380**, 243-258.
Jarzynka, M. J., Hu, B., Hui, K.-M., Bar-Joseph, I., Gu, W., Hirose, T., Haney, L. B., Ravichandran, K. S., Nishikawa, R. and Cheng, S.-Y. (2007). ELMO1 and Dock180, a bipartite Rac1 guanine nucleotide exchange factor, promote human glioma cell invasion. *Cancer Res.* **67**, 7203-7211.
Kawakami, K., Takeda, H., Kawakami, N., Kobayashi, M., Matsuda, N. and Mishina, M. (2004). A transposon-mediated gene trap approach identifies developmentally regulated genes in zebrafish. *Dev. Cell* **7**, 133-144.
Kikuta, H. and Kawakami, K. (2009). Transient and stable transgenesis using tol2 transposon vectors. *Methods Mol. Biol.* **546**, 69-84.
Kimmel, C. B., Ballard, W. W., Kimmel, S. R., Ullmann, B. and Schilling, T. F. (1995). Stages of embryonic development of the zebrafish. *Dev. Dyn.* **203**, 253-310.
Klos Dehring, D. A., Vladar, E. K., Werner, M. E., Mitchell, J. W., Hwang, P. and Mitchell, B. J. (2013). Deuterosome-mediated centriole biogenesis. *Dev. Cell* **27**, 103-112.
Kramer-Zucker, A. G., Olale, F., Haycraft, C. J., Yoder, B. K., Schier, A. F. and Drummond, I. A. (2005). Cilia-driven fluid flow in the zebrafish pronephros, brain and Kupffer's vesicle is required for normal organogenesis. *Development* **132**, 1907-1921.
Lau, L., Lee, Y. L., Sahl, S. J., Stearns, T. and Moerner, W. E. (2012). STED microscopy with optimized labeling density reveals 9-fold arrangement of a centriole protein. *Biophys. J.* **102**, 2926-2935.
Lemullois, M., Boisvieux-Ulrich, E., Laine, M.-C., Chailley, B. and Sandoz, D. (1988). Development and functions of the cytoskeleton during ciliogenesis in metazoa. *Biol. Cell* **63**, 195-208.
Link, V., Carvalho, L., Castanon, I., Stockinger, P., Shevchenko, A. and Heisenberg, C.-P. (2006). Identification of regulators of germ layer morphogenesis using proteomics in zebrafish. *J. Cell Sci.* **119**, 2073-2083.
Liu, Y., Pathak, N., Kramer-Zucker, A. and Drummond, I. A. (2007). Notch signaling controls the differentiation of transporting epithelia and multiciliated cells in the zebrafish pronephros. *Development* **134**, 1111-1122.
Madhivanan, K., Mukherjee, D. and Aguilar, R. C. (2012). Lowe syndrome: between primary cilia assembly and Rac1-mediated membrane remodeling. *Commun. Integr. Biol.* **5**, 641-644.
McClatchey, A. I. (2014). ERM proteins at a glance. *J. Cell Sci.* **127**, 3199-3204.
Mitchell, B., Jacobs, R., Li, J., Chien, S. and Kintner, C. (2007). A positive feedback mechanism governs the polarity and motion of motile cilia. *Nature* **447**, 97-101.
Mitchell, B., Stubbs, J. L., Huisman, F., Taborek, P., Yu, C. and Kintner, C. (2009). The PCP pathway instructs the planar orientation of ciliated cells in the Xenopus larval skin. *Curr. Biol.* **19**, 924-929.
Moore, C. A., Parkin, C. A., Bidet, Y. and Ingham, P. W. (2007). A role for the Myoblast city homologues Dock1 and Dock5 and the adaptor proteins Crk and Crk-like in zebrafish myoblast fusion. *Development* **134**, 3145-3153.
Murchie, R., Guo, C.-H., Persaud, A., Muise, A. and Rotin, D. (2014). Protein tyrosine phosphatase sigma targets apical junction complex proteins in the intestine and regulates epithelial permeability. *Proc. Natl. Acad. Sci. USA* **111**, 693-698.
Nigg, E. A. and Raff, J. W. (2009). Centrioles, centrosomes, and cilia in health and disease. *Cell* **139**, 663-678.
Pan, J., You, Y., Huang, T. and Brody, S. L. (2007). RhoA-mediated apical actin enrichment is required for ciliogenesis and promoted by Foxj1. *J. Cell Sci.* **120**, 1868-1876.
Parameswaran, N. and Gupta, N. (2013). Re-defining ERM function in lymphocyte activation and migration. *Immunol. Rev.* **256**, 63-79.
Park, T. J., Haigo, S. L. and Wallingford, J. B. (2006). Ciliogenesis defects in embryos lacking inturned or fuzzy function are associated with failure of planar cell polarity and Hedgehog signaling. *Nat. Genet.* **38**, 303-311.
Park, D., Tosello-Trampont, A.-C., Elliott, M. R., Lu, M., Haney, L. B., Ma, Z., Klibanov, A. L., Mandell, J. W. and Ravichandran, K. S. (2007). BAI1 is an engulfment receptor for apoptotic cells upstream of the ELMO/Dock180/Rac module. *Nature* **450**, 430-434.
Park, T. J., Mitchell, B. J., Abitua, P. B., Kintner, C. and Wallingford, J. B. (2008). Dishevelled controls apical docking and planar polarization of basal bodies in ciliated epithelial cells. *Nat. Genet.* **40**, 871-879.
Perner, B., Englert, C. and Bollig, F. (2007). The Wilms tumor genes wt1a and wt1b control different steps during formation of the zebrafish pronephros. *Dev. Biol.* **309**, 87-96.
Roubinet, C., Decelle, B., Chicanne, G., Dorn, J. F., Payrastre, B., Payre, F. and Carreno, S. (2011). Molecular networks linked by Moesin drive remodeling of the cell cortex during mitosis. *J. Cell Biol.* **195**, 99-112.
Ryser, J. E., Rungger-Brandle, E., Chaponnier, C., Gabbiani, G. and Vassalli, P. (1982). The area of attachment of cytotoxic T lymphocytes to their target cells shows high motility and polarization of actin, but not myosin. *J. Immunol.* **128**, 1159-1162.
Saotome, I., Curto, M. and McClatchey, A. I. (2004). Ezrin is essential for epithelial organization and villus morphogenesis in the developing intestine. *Dev. Cell* **6**, 855-864.
Schmidt, K. N., Kuhns, S., Neuner, A., Hub, B., Zentgraf, H. and Pereira, G. (2012). Cep164 mediates vesicular docking to the mother centriole during early steps of ciliogenesis. *J. Cell Biol.* **199**, 1083-1101.
Sorokin, S. P. (1968). Reconstructions of centriole formation and ciliogenesis in mammalian lungs. *J. Cell Sci.* **3**, 207-230.
Steinman, R. M. (1968). An electron microscopic study of ciliogenesis in developing epidermis and trachea in the embryo of Xenopus laevis. *Am. J. Anat.* **122**, 19-55.
Stinchcombe, J. C., Majorovits, E., Bossi, G., Fuller, S. and Griffiths, G. M. (2006). Centrosome polarization delivers secretory granules to the immunological synapse. *Nature* **443**, 462-465.
Tissir, F., Qu, Y., Montcouquiol, M., Zhou, L., Komatsu, K., Shi, D., Fujimori, T., Labeau, J., Tyteca, D., Courtoy, P. et al. (2010). Lack of cadherins Celsr2 and Celsr3 impairs ependymal ciliogenesis, leading to fatal hydrocephalus. *Nat. Neurosci.* **13**, 700-707.
Turunen, O., Wahlström, T. and Vaheri, A. (1994). Ezrin has a COOH-terminal actin-binding site that is conserved in the ezrin protein family. *J. Cell Biol.* **126**, 1445-1453.
Viswanatha, R., Ohouo, P. Y., Smolka, M. B. and Bretscher, A. (2012). Local phosphocycling mediated by LOK/SLK restricts ezrin function to the apical aspect of epithelial cells. *J. Cell Biol.* **199**, 969-984.
Wallmeier, J., Al-Mutairi, D. A., Chen, C.-T., Loges, N. T., Pennekamp, P., Menchen, T., Ma, L., Shamseldin, H. E., Olbrich, H., Dougherty, G. W. et al. (2014). Mutations in CCNO result in congenital mucociliary clearance disorder with reduced generation of multiple motile cilia. *Nat. Genet.* **46**, 646-651.
Werner, M. E. and Mitchell, B. J. (2012). Understanding ciliated epithelia: the power of Xenopus. *Genesis* **50**, 176-185.
Werner, M. E., Hwang, P., Huisman, F., Taborek, P., Yu, C. C. and Mitchell, B. J. (2011). Actin and microtubules drive differential aspects of planar cell polarity in multiciliated cells. *J. Cell Biol.* **195**, 19-26.
Werner, M. E., Mitchell, J. W., Putzbach, W., Bacon, E., Kim, S. K. and Mitchell, B. J. (2014). Radial intercalation is regulated by the Par complex and the microtubule-stabilizing protein CLAMP/Spef1. *J. Cell Biol.* **206**, 367-376.
Westerfield (1995). *The Zebrafish Book: A Guide for the Laboratory Use of Zebrafish (Danio rerio)*. Eugene: University of Oregon Press.
Zhu, L., Hatakeyama, J., Chen, C., Shastri, A., Poon, K. and Forte, J. G. (2008). Comparative study of ezrin phosphorylation among different tissues: more is good; too much is bad. *Am. J. Physiol. Cell Physiol.* **295**, C192-C202.